

MASTER COPY: PLEASE KEEP THIS "MEMORANDUM OF TRANSMITTAL" BLANK FOR REPRODUCTION PURPOSES. WHEN REPORTS ARE GENERATED UNDER THE ARO SPONSORSHIP, FORWARD A COMPLETED COPY OF THIS FORM WITH EACH REPORT SHIPMENT TO THE ARO. THIS WILL ASSURE PROPER IDENTIFICATION. NOT TO BE USED FOR INTERIM PROGRESS REPORTS; SEE PAGE 2 FOR INTERIM PROGRESS REPORT INSTRUCTIONS.

MEMORANDUM OF TRANSMITTAL

U.S. Army Research Office
ATTN: AMSRL-RO-BI (TR)
P.O. Box 12211
Research Triangle Park, NC 27709-2211

Reprint (Orig + 2 copies)

Technical Report (Orig + 2 copies)

Manuscript (1 copy)

Final Progress Report (Orig + 2 copies)

Related Materials, Abstracts, Theses (1 copy)

CONTRACT/GRANT NUMBER:

REPORT TITLE:

is forwarded for your information.

SUBMITTED FOR PUBLICATION TO (applicable only if report is manuscript):

Sincerely,

REPORT DOCUMENTATION PAGE

Form Approved
OMB NO. 0704-0188

Public Reporting burden for this collection of information is estimated to average 1 hour per response, including the time for reviewing instructions, searching existing data sources, gathering and maintaining the data needed, and completing and reviewing the collection of information. Send comment regarding this burden estimates or any other aspect of this collection of information, including suggestions for reducing this burden, to Washington Headquarters Services, Directorate for information Operations and Reports, 1215 Jefferson Davis Highway, Suite 1204, Arlington, VA 22202-4302, and to the Office of Management and Budget, Paperwork Reduction Project (0704-0188,) Washington, DC 20503.

1. AGENCY USE ONLY (Leave Blank)	2. REPORT DATE	3. REPORT TYPE AND DATES COVERED	
4. TITLE AND SUBTITLE		5. FUNDING NUMBERS	
6. AUTHOR(S)		8. PERFORMING ORGANIZATION REPORT NUMBER	
7. PERFORMING ORGANIZATION NAME(S) AND ADDRESS(ES)		10. SPONSORING / MONITORING AGENCY REPORT NUMBER	
9. SPONSORING / MONITORING AGENCY NAME(S) AND ADDRESS(ES) U. S. Army Research Office P.O. Box 12211 Research Triangle Park, NC 27709-2211		11. SUPPLEMENTARY NOTES The views, opinions and/or findings contained in this report are those of the author(s) and should not be construed as an official Department of the Army position, policy or decision, unless so designated by other documentation.	
12 a. DISTRIBUTION / AVAILABILITY STATEMENT Approved for public release; distribution unlimited.		12 b. DISTRIBUTION CODE	
13. ABSTRACT (Maximum 200 words)			
14. SUBJECT TERMS			15. NUMBER OF PAGES
17. SECURITY CLASSIFICATION OR REPORT UNCLASSIFIED			16. PRICE CODE
18. SECURITY CLASSIFICATION ON THIS PAGE UNCLASSIFIED		19. SECURITY CLASSIFICATION OF ABSTRACT UNCLASSIFIED	20. LIMITATION OF ABSTRACT UL

NSN 7540-01-280-5500

Standard Form 298 (Rev.2-89)
Prescribed by ANSI Std. 239-18
298-102

Transmission Range Optimization for FH-CDMA Networks in Time-Varying Channels

Haichang Sui and James R. Zeidler

Dept. of Electrical & Computer Engineering,
Univ. of California, San Diego, La Jolla, CA 92093-0407
Emails: haichangsui@gmail.com, zeidler@ece.ucsd.edu

ABSTRACT

Abstract— Optimization of the transmission range for maximizing information efficiency is studied in this paper for mobile ad hoc networks with frequency-hopped (FH) CDMA and multiple antennas. Realistic channel models are employed to account for path-loss, log-normal shadowing, and Rayleigh fading. The shadowing and fading are assumed time-varying with different time-scales. The receiver performs decision-feedback demodulation for differential unitary space-time modulation and erasure insertion decoding for Reed-Solomon codes. The decoding error probability is derived based on distributions of the multiple access interference power and the SIR for ground propagation model (path-loss exponent equal to 4). The trade-off between information efficiency and transmission range is studied in detail and insight is obtained into the impact of various system parameters.

An important design issue in mobile ad hoc wireless networks is to determine the optimum transmission range [1]. For networks where nodes are randomly distributed on the plane according to a two-dimensional Poisson distribution with density λ , the transmission range R can be specified by $N_0 \triangleq \lambda\pi R^2$, which is related to network connectivity [1]. Optimizing R , or N_0 equivalently, has been studied for such networks with slotted ALOHA protocol in previous literature [2]-[6] [8]. For maximizing the expected forward progress, it is shown that the optimum N_0 scales with the spreading gain in DSCDMA networks where nodes are equipped with single-user receivers and no power control is employed [2], [3]. On the other hand, more insight into network design may be revealed by considering the product of the expected forward progress and the spectral efficiency, or the so-called *information efficiency* (IE) [4]. Optimizing

N_0 to maximize IE for DS-CDMA networks is studied in [4] for a channel with no shadowing. Compared to DS-CDMA, an important feature of frequency-hopped (FH) CDMA is that, due to hopping and interleaving, the coded symbols corresponding to the same codeword are subject to different SINR levels. Such “interference diversity” can be exploited by proper coding and interleaving to effectively suppress MAI [8]-[11]. In contrast, symbols in the same packet are usually subject to the same SINR level in narrow-band or DS-CDMA networks and the packet error probability is commonly determined by a threshold test on the SINR [2], [3], [4], [7]. This makes FH-CDMA very robust to the near-far problem, while DS-CDMA requires either accurate power-control or multi-user detection.

A Reed-Solomon (RS) coded FH-CDMA transceiver with MIMO is developed in [10], [11], where differential unitary space-time modulation (DUSTM) is used to achieve spatial diversity noncoherently. Decision-feedback demodulation (DFD), decision-directed adaptive estimation, and erasure insertion (EI) decoding operate interactively to mitigate time-varying fading, estimate symbol reliability, and suppress interference. The superior near-far resistance observed in [10], [11] motivates us to further investigate transmission range optimization with the proposed FH transceiver for maximizing IE. Previous studies of similar problems include [5], [6], which consider FSK and RS coding without EI. Other related works include [8], [9], where bit-interleaved coded modulation and coherent demodulation are assumed.

Our study assumes a realistic time-varying channel model, which accounts for path-loss, log-normal shadowing, and Rayleigh fading. Different time-scales are used to model the time-variation of different channel effects. Results in this paper extend previous studies [2]-[9] to include the impact of the time-varying fading

⁰This work is supported by, or in part by, the Office of Naval Research (Code 313) and the U. S. Army Research Office under the Multi-University Research Initiative (MURI) grant # W911NF-04-1-0224.

and shadowing on network design. The optimum N_0 for maximizing IE is shown to be linearly proportional to the spreading gain q in FH-CDMA networks, while it scales as \sqrt{q} in DS-CDMA networks without multi-user detection or power-control. The trade-off between transmission range and IE critically depends on the modulation and coding scheme (MCS). Optimum MCSs are found for different system settings by numerical analysis, which offers guidance for adaptive transmissions from a network perspective. Our results further shed light on how the network performance depends on various design parameters and channel properties, including the number of antennas, receiver configuration, dwell length, Doppler frequency, and shadowing spread/speed.

The rest of the paper is organized as follows. The system model is presented in Section I. In Section II, packet error probability and IE are derived. The trade-off between IE and the transmission range, together with the effects of various system parameters, are studied in detail in Section III and Section IV concludes the paper.

I. SYSTEM MODEL

A. Network Model

We consider a network where nodes are randomly distributed over the plane according to a two-dimensional Poisson process with density λ and access the channel according to the slotted-ALOHA protocol with transmission probability p . The transmitting and receiving nodes of interest are denoted by \mathcal{S} and \mathcal{D} respectively, which are separated by the transmission range R . AWGN is ignored and the transmit power of all nodes is set to be unity [5]. Random hopping patterns are assumed in this paper. The total number of carrier frequencies that a hopped signal can be transmitted on, i.e. the spreading gain, is denoted by q .

B. Transceiver and Channel Model (PHY)

The PHY transceiver structure is specified in detail in [10], [11]. At the transmitter shown in Fig.1, information bits are coded by (L, K) RS code and the coded symbols are then modulated by DUSTM. For simplicity, we assume the codeword length L is also the size of the DUSTM constellation $\mathcal{V} = \{\mathbf{V}_0, \dots, \mathbf{V}_{L-1}\}$, where $\{\mathbf{V}_l\}_{l=0}^{L-1}$ are $N_T \times N_T$ unitary matrices and N_T is the number of transmit antennas. By denoting the τ th coded symbol as z_τ ($z_\tau = 0, \dots, L-1$), the corresponding space-time signal to be transmitted is an $N_T \times N_T$ unitary matrix generated by differential modulation $\mathbf{S}_{0,\tau} = \mathbf{V}_{z_\tau} \mathbf{S}_{0,\tau-1}$. The length of a DUSTM block is denoted by T_s and $\mathbf{S}_{0,\tau}$ is transmitted in the τ th block by one of

the q carrier frequencies. The hopping rate is assumed to be $\frac{1}{N_c T_s}$ for some positive integer $N_c > 1$ (slow FH) and the interval between hops is referred as a dwell. The interleaver and packet format are the same as in [5], [10], [11]. Specifically, a packet contains multiple frames while each frame consists of N_c RS codewords, which are interleaved such that the L coded symbols from the same codeword are transmitted in different dwells to achieve frequency diversity.

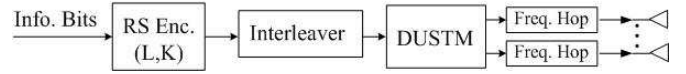


Fig. 1. Transmitter model

The wireless channel between two arbitrary nodes is subject to deterministic path-loss and time-varying shadowing and fading. Formally, the channel gain can be written as $d^{-b/2} \cdot \sqrt{S(t)} \cdot h(t)$ where d is the distance between the two nodes, b is the path-loss exponent, $S(t)$ is a log-normal r.v. representing shadowing, and $h(t)$ is circular symmetric complex (c.s.c.) Gaussian due to Rayleigh fading. The pdf of $S(t)$ is given by

$$f_S(s) = \frac{1}{\sqrt{2\pi}\sigma_s s} e^{-\frac{\ln^2 y}{2\sigma_s^2}}, \quad (1)$$

where $\frac{10}{\ln 10} \sigma_s$ is the shadowing spread expressed in decibel. The received space-time signal \mathbf{R}_τ in the τ th DUSTM block after dehopping can be written as an $N_T \times N_R$ matrix. If the shadowing $S_0(t)$ and the fading $h_0(t)$ between \mathcal{S} and \mathcal{D} are assumed time-invariant within each DUSTM block of length T_s , we have

$$\mathbf{R}_\tau = R^{-b/2} \sqrt{S_0(\tau)} \mathbf{S}_{0,\tau} \mathbf{H}_{0,\tau} + \mathbf{R}_{MAI,\tau}, \quad (2)$$

where $\mathbf{R}_{MAI,\tau}$ represents MAI, and the $N_T \times N_R$ channel matrix $\mathbf{H}_{0,\tau}$ contains the Rayleigh fading coefficients between all $N_T N_R$ antenna pairs, which are i.i.d. c.s.c. Gaussian r.v.s with zero mean and unit variance.

The receiver proposed in [10], [11] performs DFD, decision-directed adaptive estimation, and EI decoding interactively, as shown in Fig.2. The DFD demodulate the transmitted symbol z_τ by $\hat{z}_\tau = \arg \max_{k=0, \dots, L-1} \lambda_{\tau,k}$ [10], [11], where

$$\lambda_{\tau,k} = \frac{1}{\hat{\sigma}_{P,\tau}^2} \left\| \mathbf{V}_k^H \mathbf{R}_\tau - \sum_{j=1}^P \hat{a}_{j,\tau} \left(\prod_{t=\tau-j+1}^{\tau-1} \mathbf{V}_{\hat{z}_t} \right) \mathbf{R}_{\tau-j} \right\|^2. \quad (3)$$

The coefficients $\hat{a}_{1,\tau}, \dots, \hat{a}_{P,\tau}$ and $\hat{\sigma}_{P,\tau}^2$ in (3) are adaptively updated by the decision-directed RLS algorithm in

Fig.2. Details of the algorithm can be found in [10], [11] and will not be presented here. In this paper, EI based on the so-called *effective SIR* (ESIR) [10] is considered. The ESIR accounts for the time-correlation of Rayleigh fading and the feedback length P , which is given by [17]

$$\rho_{\text{eff}}(\rho) = (P_R + \sigma_w^2) / \sigma_P^2 - 1, \quad (4)$$

where $P_R \triangleq R^{-b} S_0$ is the received signal power and σ_P^2 is the P -th order minimum linear prediction error variance of the Gaussian random process $\{\mathbf{H}_{0,\tau} + \mathbf{R}_{MAI,\tau}\}_\tau$. The value of σ_P^2 and the theoretical values of $\hat{a}_{1,\tau}, \dots, \hat{a}_{P,\tau}$ can be solved from the Yule-Walker equations (c.f. [17] (8)). In practice, it is estimated by $\hat{\rho}_{\text{eff},\tau} \triangleq \frac{\hat{P}_{\text{tot},\tau}}{\hat{\sigma}_{P,\tau}^2} - 1$ where $\hat{P}_{\text{tot},\tau} = \mu \hat{P}_{\text{tot},\tau-1} + \frac{1-\mu}{N_T N_R} \|\mathbf{R}_\tau\|^2$ is an estimate of total received signal plus interference power [10] and μ is the forgetting factor. The demodulated symbol \hat{z}_τ is erased if $\hat{\rho}_{\text{eff},\tau} \leq \rho_{\text{eth}}$ is satisfied. Since the reliability of DFD can be measured by the ESIR [17], the decoding error probability may be significantly improved by choosing ρ_{eth} appropriately [10]. The IE with and without the ESIR threshold test (ESTT) EI will be analyzed in Section II.

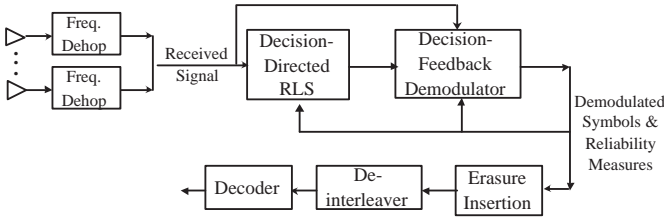


Fig. 2. Receiver model

An important consideration in performance analysis is the time-variation of the channel. The relative distance between nodes is assumed invariant at least in a packet duration. The Rayleigh fading is time-varying across DUSTM blocks with time-correlation parameterized by the normalized Doppler frequency $f_d T_s$ according to Jakes' model. We consider two different time-scales for shadowing, which generally has less time-variation than Rayleigh fading. In *fast shadowing*, $S_0(\tau)$ is assumed constant in a dwell and independent across dwells. In *slow shadowing*, $S_0(\tau)$ is assumed to be constant for the whole packet as in [5], [6], [8]. It is clear that whether the shadowing is fast or slow time-varying depends not only on the mobility but also on the length of a dwell.

C. Interference Model

For clarity, we assume dwell synchronization so that the MAI process $\{\mathbf{R}_{MAI,\tau}\}_\tau$ is stationary in a dwell.

The MAI $\mathbf{R}_{MAI,\tau}$ can be formally defined as $\mathbf{R}_{MAI,\tau} = \lim_{a \rightarrow \infty} \mathbf{R}_{MAI,\tau}(a)$, where $\mathbf{R}_{MAI,\tau}(a)$ denotes the MAI resulted from nodes in a circle centered at node \mathcal{D} with radius a , which is given by

$$\mathbf{R}_{MAI,\tau}(a) = \sum_k^{[\lambda' \pi a^2]} d_k^{-b/2} \sqrt{S_k(\tau)} \mathbf{S}_{k,\tau} \mathbf{H}_{k,\tau}. \quad (5)$$

In (5), the notation $\sum^{[N'_0]}$ refers to a sum whose number of terms is a Poisson r.v. with mean N'_0 and $\lambda' \triangleq \lambda p/q$ is the density of interfering nodes. The r.v. d_k and $S_k(\tau)$ in (5) are the distance and log-normal shadowing (with pdf (1)) of the k th interferer- \mathcal{D} link respectively. The interference signal $\mathbf{S}_{k,\tau}$ is $N_T \times N_{T,k}$ and the Rayleigh fading matrix $\mathbf{H}_{k,\tau}$ is $N_{T,k} \times N_R$. Gaussian approximation is employed for elements in $\mathbf{S}_{k,\tau} \mathbf{H}_{k,\tau}$, whose variance is normalized to unity to account for equal transmit power of nodes. It is further assumed that $\mathbf{S}_{k,\tau} \mathbf{H}_{k,\tau}$ are independent for different k s and uncorrelated in space and time. Thus, by conditioning on the distance and shadowing for all interferer- \mathcal{D} links, elements in $\mathbf{R}_{MAI,\tau}(a)$ are i.i.d. c.s.c. Gaussian r.v.s with zero mean and variance given by

$$\sigma_w^2(a) \triangleq \sum_k^{[\lambda' \pi a^2]} d_k^{-b} S_k. \quad (6)$$

In (6), time dependence of the shadowing is not explicitly shown because it is constant within a dwell in both the fast and slow shadowing model. The MAI process $\{\mathbf{R}_{MAI,\tau}\}_\tau$ in a dwell is thus modelled to be stationary c.s.c. Gaussian and uncorrelated in space/time when conditioned on its variance

$$\sigma_w^2 \triangleq \lim_{a \rightarrow \infty} \sigma_w^2(a), \quad (7)$$

which is itself an i.i.d. r.v. for each dwell. Distribution of σ_w^2 will be derived in Section II-B.

II. INFORMATION EFFICIENCY AND OPTIMUM TRANSMISSION RANGE

In this section, we use IE as the objective function to optimize the transmission range R , or $N_0 = \lambda \pi R^2$ equivalently. The IE is defined in [5] as

$$IE \triangleq \tau(p) \cdot (1 - P_E) \cdot \xi \cdot R, \quad (8)$$

where $\tau(p) = (1-p)(1-e^{-p})$ is the “*tendency to pair-up*” [2]. In (8), $\xi = \frac{1}{q} \frac{K}{L} \log_2(L)$ is the spectral efficiency (bits/sec/Hz). The packet error probability is denoted by P_E in (8) and will be approximated by the decoding error probability P_C .

In the rest of this section, we will first review the results on ESIR and symbol error probability derived in [17] by conditioning on the received SIR $\rho \triangleq \frac{R^{-b}S_0}{\sigma_w^2}$, where S_0 and σ_w^2 are the shadowing and MAI power in a given dwell. Then the pdf of σ_w^2 is derived. Finally, the distribution of ρ is derived and the decoding error probability P_C is obtained based on the resulting distribution and the conditional symbol error/erasure probabilities.

A. Symbol error/erasure probability

When feedback errors are ignored, the pairwise error probability is given in [17] by

$$\begin{aligned} P_{k,l}(\rho) &\triangleq \Pr\{\widehat{z}_\tau = k | z_\tau = l\} \\ &= \frac{1}{\pi} \int_0^{\pi/2} \prod_{m=1}^{N_T} \left[1 + \frac{\rho_{\text{eff}}(\rho) \sigma_{m,k,l}^2}{4 \cos^2 \theta} \right]^{-N_R} d\theta \quad (9) \end{aligned}$$

where $\sigma_{m,k,l}$ ($m = 1, \dots, N_T$) is the m th singular value of the matrix $\mathbf{V}_k - \mathbf{V}_l$. The pre-EI symbol error probability can be approximated by the union bound as $P_e(\rho) \cong \frac{1}{L} \sum_{l=0}^{L-1} \sum_{k=0, k \neq l}^{L-1} P_{k,l}(\rho)$.

For the purpose of analysis, the ESTT EI is equivalent to a threshold test on ρ with a certain threshold $\rho_{\text{th}} > 0$. The post-EI symbol error and erasure probabilities can be expressed as

$$P_a(\rho, \rho_{\text{th}}) = \begin{cases} 1, & \rho \leq \rho_{\text{th}} \\ 0, & \rho > \rho_{\text{th}} \end{cases} \quad (10)$$

$$P_e(\rho, \rho_{\text{th}}) = \begin{cases} 0, & \rho \leq \rho_{\text{th}} \\ P_e(\rho), & \rho > \rho_{\text{th}} \end{cases} \quad (11)$$

The analytic decoding error probability of ESTT EI based on (10), (11) is shown to be in good accuracy with link simulation results, where the estimated ESIR is used for EI [10]. The optimum threshold test is also derived in [10] for EI and shown to be robust to the choice of threshold. Results in [10] further showed that analysis of ESTT EI with optimized ρ_{th} is close to the performance of the optimum EI in interference dominated environment. This justifies the network analysis based on ESTT EI with optimized threshold in this paper.

B. Distribution of the MAI power

Due to the nature of Poisson processes on a plane, interfering nodes are uniformly distributed in a circle centered at \mathcal{D} with an arbitrary radius a [13]. That is, the pdf of d_k in (6) is given by

$$f_d(r) = \frac{2r}{a^2} \quad (r \leq a). \quad (12)$$

In the following, we derive $\phi_{\text{MAI}}(\omega)$, the characteristic function (CF) of σ_w^2 , based on the influence function method [13]. Results in [13], [14], [15] cannot be directly applied to obtain the CF of σ_w^2 considered in this paper because the log-normal r.v. S_k in (6) is neither zero-mean nor spherically symmetric.

By definition, we can write $\phi_{\text{MAI}}(\omega) = \mathbb{E}[e^{j\omega\sigma_w^2}]$ as

$$\phi_{\text{MAI}}(\omega) = \lim_{a \rightarrow \infty} \mathbb{E} \left\{ \exp \left(j\omega \sum_k^{\lfloor \lambda' \pi a^2 \rfloor} d_k^{-b} S_k \right) \right\}. \quad (13)$$

Since d_k, S_k are i.i.d. and the number of terms in (13) is a Poisson r.v., we have

$$\begin{aligned} \phi_{\text{MAI}}(\omega) &= \lim_{a \rightarrow \infty} \sum_{m=0}^{\infty} \frac{(\lambda' \pi a^2)^m \mathbb{E}^m [\exp(j\omega d^{-b} S)]}{e^{\lambda' \pi a^2} m!} \\ &= \lim_{a \rightarrow \infty} \exp \left\{ \lambda' \pi a^2 \left[\mathbb{E} \left(e^{j\omega d^{-b} S} \right) - 1 \right] \right\}. \quad (14) \end{aligned}$$

By denoting the CF of S to be $\phi_S(\cdot)$ and integrating by part, the expectation in (14) becomes

$$\begin{aligned} \mathbb{E} \left(e^{j\omega d^{-b} S} \right) &= \phi_S(a^{-b}\omega) - \lim_{r \rightarrow 0} \frac{r^2}{a^2} \phi_S(r^{-b}\omega) \\ &\quad - \int_0^a \frac{r^2}{a^2} \frac{d\phi_S(r^{-b}\omega)}{dr} dr. \quad (15) \end{aligned}$$

The second term in (15) is zero if $\phi_S(\omega)$ is bounded for arbitrary ω . Furthermore, by changing variables and applying L'Hopital's rule, we have

$$\lim_{a \rightarrow \infty} \lambda' \pi a^2 \left[\phi_S(a^{-b}\omega) - 1 \right] = \frac{\lambda' \pi j \omega}{2} \mathbb{E}[S] \lim_{x \rightarrow 0} x^{b-2}. \quad (16)$$

If we assume the path-loss exponent satisfies $b > 2$, we have the following from (14)-(16):

$$\phi_{\text{MAI}}(\omega) = \exp \left(\lambda' \pi \int_0^\infty \frac{d\phi_S(t\omega)}{dt} t^{-2/b} dt \right) \quad (17)$$

By denoting $\alpha = 2/b$ and noticing that $\mathbb{E}[S^\alpha] = \exp\left(\alpha^2 \frac{\sigma_s^2}{2}\right)$ for log-normal r.v. S , the integral in (17) can be further simplified as

$$\begin{aligned} \int_0^\infty \frac{d\phi_S(t\omega)}{dt} t^{-\alpha} dt &= j\omega \mathbb{E} \left[S \int_0^\infty e^{jSt\omega} t^{-\alpha} dt \right] \\ &= -\Gamma(1-\alpha) (-j\omega)^\alpha \mathbb{E}[S^\alpha] \quad (18) \end{aligned}$$

where $\Gamma(x)$ is the Gamma function. Consequently, the CF of σ_w^2 for $b > 2$ reduces to

$$\begin{aligned} \ln \phi_{\text{MAI}}(\omega) &= -\lambda' \pi \Gamma(1-\alpha) e^{\frac{1}{2} \alpha^2 \sigma_s^2} \cos \frac{\alpha \pi}{2} |\omega|^\alpha \\ &\quad \times \left[1 - j \operatorname{sgn}(\omega) \tan \frac{\alpha \pi}{2} \right], \quad (19) \end{aligned}$$

from which it is clear that σ_w^2 is an alpha-stable r.v. [12].

Unfortunately, the pdf of σ_w^2 can be expressed in closed-form only when $b = 4$, in which case the distribution coincides with the Levy distribution, whose pdf and the cumulative distribution function (cdf) are

$$f_{\text{MAI}}(x) = \frac{\gamma x^{-\frac{3}{2}} e^{-\frac{\gamma}{2x}}}{\sqrt{2\pi}}, \quad F_{\text{MAI}}(x) = \text{erfc}\left(\frac{\gamma}{\sqrt{2x}}\right), \quad (20)$$

for $x \geq 0$ with $\gamma \triangleq \lambda\pi^{3/2}e^{\sigma_s^2/8}/\sqrt{2}$. We will focus on the ground wave propagation model ($b = 4$) in the sequel.

C. Decoding error probability

The decoding error probability under EI is

$$P_C = \sum_{i=0}^L \sum_{j=j_0(i)}^{L-i} \frac{L! \bar{P}_e^i \bar{P}_a^j (1 - \bar{P}_e - \bar{P}_a)^{L-i-j}}{i!j!(L-i-j)!} \quad (21)$$

where $j_0(i) \triangleq \max(L - K + 1 - 2i, 0)$ and \bar{P}_a, \bar{P}_e are the probabilities of demodulated symbols being erased or erroneous, respectively. \bar{P}_a, \bar{P}_e can be obtained by averaging (10), (11) over the distribution of ρ , which is derived in the next for slow and fast shadowing.

1) *Slow shadowing*: In slow shadowing, transmitted symbols corresponding to the same codeword experience the same realization of log-normal shadowing. Therefore, the symbol erasure/error probabilities have to be derived by conditioning on the shadowing first. The average decoding error probability is then obtained by averaging over the log-normal distribution (1).

Based on (20) and conditioning on S_0 , it is easy to derive the pdf and cdf of ρ to be

$$f_{\rho|S_0}(t) = \frac{N'_0 e^{\sigma_s^2/8}}{2\sqrt{S_0 t}} \exp\left(-\frac{N'_0{}^2 \pi e^{\sigma_s^2/4}}{4S_0} t\right), \quad (22)$$

$$F_{\rho|S_0}(t) = \text{erf}\left(\frac{N'_0 e^{\sigma_s^2/8}}{2} \sqrt{\frac{\pi t}{S_0}}\right), \quad (23)$$

where $N'_0 \triangleq \lambda' \pi R^2 = \frac{p}{q} N_0$. By averaging (10), (11) over the distribution (22), we have

$$\bar{P}_{a|S_0}(\rho_{\text{th}}) = \text{erf}\left(\frac{N'_0 e^{\sigma_s^2/8}}{2} \sqrt{\frac{\pi}{S_0} \rho_{\text{th}}}\right), \quad (24)$$

$$\bar{P}_{e|S_0}(\rho_{\text{th}}) = \int_{\rho > \rho_{\text{th}}} \frac{N'_0 e^{\frac{\sigma_s^2}{8} - \frac{N'_0{}^2 \pi e^{\sigma_s^2/4}}{4S_0} \rho}}{2\sqrt{S_0 \rho}} P_e(\rho) d\rho. \quad (25)$$

The decoding error probability conditioned on S_0 is thus

$$P_{C|S_0}(\rho_{\text{th}}) = \sum_{i=0}^L \sum_{j=j_0(i)}^{L-i} \frac{L! \bar{P}_{e|S_0}^i(\rho_{\text{th}}) \bar{P}_{a|S_0}^j(\rho_{\text{th}})}{i!j!(L-i-j)!} \times [1 - \bar{P}_{e|S_0}(\rho_{\text{th}}) - \bar{P}_{a|S_0}(\rho_{\text{th}})]^{L-i-j} \quad (26)$$

By optimizing over ρ_{th} , we get $P_{C|S_0} = \min_{\rho_{\text{th}}} P_{C|S_0}(\rho_{\text{th}})$. The decoding error probability is obtained by

$$P_C = E_{S_0} [P_{C|S_0}] = \frac{1}{\sqrt{\pi}} \int_{-\infty}^{\infty} e^{-z^2} P_{C|e^{\sqrt{2}\sigma_s z}} dz. \quad (27)$$

2) *Fast shadowing*: In fast shadowing, the SIR in a given dwell has a pdf $f_{\rho}(t) = E_{S_0} [f_{\rho|S_0}(t)]$ where $f_{\rho|S_0}(t)$ is given in (22). By applying Gaussian quadrature rule with Hermite polynomials again, we have

$$f_{\rho}(t) = \int_{-\infty}^{\infty} \frac{1}{\sqrt{2\pi\sigma_s}} e^{-\frac{x^2}{2\sigma_s^2}} f_{\rho|e^x}(t) dx \cong \frac{N'_0 e^{\sigma_s^2/4}}{2\sqrt{\pi t}} \sum_{n=1}^{N_p} H_{x_n} e^{-\frac{\pi}{4} N'_0{}^2 e^{3\sigma_s^2/4} - \sqrt{2}\sigma_s x_n t} \quad (28)$$

Based on (28), the symbol erasure probability is

$$\bar{P}_a(\rho_{\text{th}}) = \int_0^{\rho_{\text{th}}} f_{\rho}(t) dt. \quad (29)$$

and the post-EI symbol error probability is

$$\bar{P}_e(\rho_{\text{th}}) = \int_{\rho > \rho_{\text{th}}} P_e(\rho) f_{\rho}(\rho) d\rho \quad (30)$$

The decoding error probability is again given by $P_C = \min_{\rho_{\text{th}}} P_C(\rho_{\text{th}})$ where $P_C(\rho_{\text{th}})$ is given by (21).

D. Optimizing IE

From the analysis in Section II-C, we notice that the decoding error probability depends on

$$N'_0 = \frac{p}{q} N_0. \quad (31)$$

After some manipulation, we can write

$$\sqrt{\lambda} IE = \frac{\tau(p) \log_2(L) K}{\sqrt{\pi p} \sqrt{q}} \frac{1}{L} [1 - P_C(N'_0)] \sqrt{N'_0} \quad (32)$$

The optimal ALOHA transmission probability is given by $p_{\text{opt}} = \arg \max_p \frac{\tau(p)}{\sqrt{\pi p}} = 0.27$, which is consistent with [2], [3], [5].

The role of spreading gain q can be readily observed from (31) and (32). Specifically, when other parameters are fixed in (32), the optimal N_0 is proportional to q due to (31), while the maximum achievable IE is inversely proportional to \sqrt{q} . This is in contrast with the results obtained in [2] [3] for DS-CDMA networks with single-user receiver and no power-control, where the authors showed that the optimum N_0 is proportional to \sqrt{q} . The corresponding IE is therefore on the order of $\frac{1}{q} \cdot q^{\frac{1}{4}} = q^{-\frac{3}{4}} < q^{-\frac{1}{2}}$. This may suggest the advantage of FH-CDMA over DS-CDMA in terms of both the transmission range and the IE, when the total bandwidth constraint is the same for both. Such an

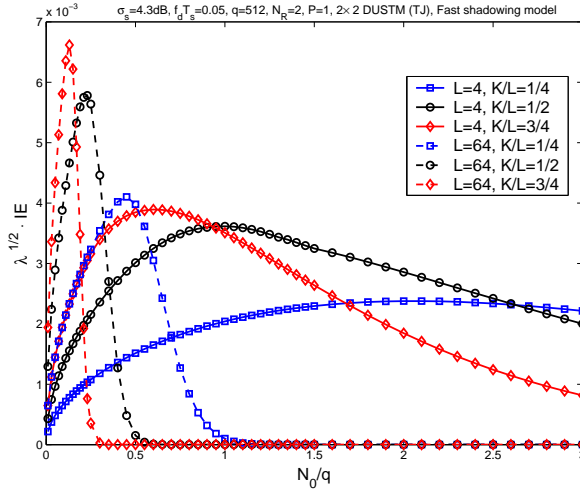


Fig. 3. $\sqrt{\lambda}IE$ versus $\frac{N_0}{q}$ for different MCSs ($N = 2$, $P = 1$, $\sigma_s = 4.3\text{dB}$, fast shadowing, $f_d T_s = 0.05$)

advantage comes from the inherent near-far resistance of FH-CDMA waveform compared to DS-CDMA with single-user receiver and no power control.

III. NUMERICAL RESULTS

In this section, the trade-off between $\sqrt{\lambda}IE$ and $\frac{N_0}{q}$ together with the impact of various parameters are studied in more detail. We set $q = 512$ as a baseline for comparison, but as discussed in Section II-D, the results can be easily interpreted for other values of q . Two transmit antennas are considered in simulation and the DUSTM constellations proposed in [16] are employed. Also $p_{\text{opt}} = 0.27$ is always assumed.

In Fig.3, curves of $\sqrt{\lambda}IE$ versus $\frac{N_0}{q}$ are plotted for DUSTM constellation size 4 and 64 with code rate $\frac{1}{4}$, $\frac{1}{2}$, $\frac{3}{4}$, respectively. It is observed that the MCS impacts the trade-off significantly. Observed from the peaks of the curves in Fig.3, lower maximum IE is achieved as the code rate or constellation size decreases.

The next two figures shows the effects of different channels. Curves in Fig.4 correspond to different shadowing models. The maximum achievable IE is higher for fast shadowing than for slow shadowing because higher time diversity is available under the fast shadowing model. Interestingly, the comparison reverses as the transmission range extends beyond a certain point and the MAI becomes more dominant. This is mainly because, in fast shadowing, multiple independent shadowing realizations have to meet certain SIR threshold for a packet to be successfully decoded, while the packet is subject to the same shadowing in slow shadowing and the probability of satisfying certain SIR requirement

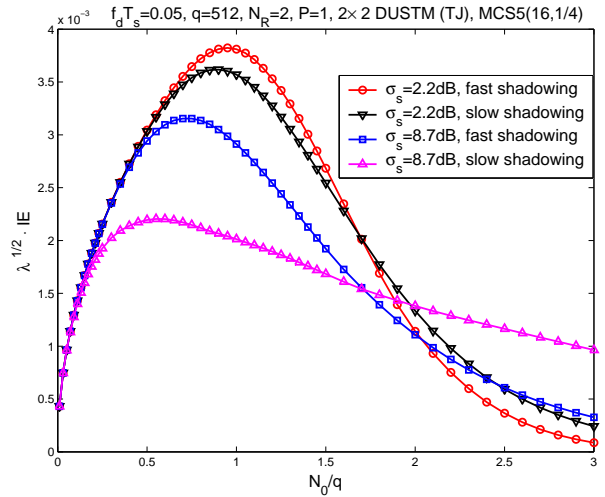


Fig. 4. $\sqrt{\lambda}IE$ versus $\frac{N_0}{q}$ for different shadowing models ($L = 16$, $K/L = \frac{1}{4}$, $N = 2$, $P = 1$, $f_d T_s = 0.05$)

can be much greater for a single shadowing realization than for multiple realizations when the interference is dominant. In terms of dwell length, this indicates that whether long or short dwell is advantageous depends on the transmission range among other factors. As expected, the gap between the fast and slow shadowing is reduced as σ_s decreases and the shadowing becomes more deterministic.

The effect of different mobility is shown in Fig.5. It is observed that higher mobility results in lower maximum achievable IE and reduced optimum transmission range. However, the performance may be significantly improved by increasing the DFD feedback length P to alleviate the time-varying Rayleigh fading. It is further shown in Fig.6 that the spatial diversity from receive antenna array and interference suppression capability from EI are very valuable for improving the network performance, which corroborates their importance in the link performance reported in [10], [11].

IV. CONCLUSION

In this paper, information efficiency and transmission range optimization is studied for FH-CDMA ALOHA networks with randomly distributed nodes. The MIMO transceiver proposed in [10], [11] is considered, where RS codes and DUSTM are employed with DFD and EI decoding. The time-varying channel between any two nodes is subject to path-loss, log-normal shadowing, and Rayleigh fading. We have shown that the expected number of nodes in the optimum transmission range and the corresponding maximum information efficiency

are proportional to q and $q^{-1/2}$ respectively, where q is the spreading gain. This implies higher information efficiency and increased transmission range for FH-CDMA relative to DS-CDMA networks at large spreading gain when a single-user receiver is used without power control. It is also shown that the performance critically depend on the MCS. Insight is obtained into optimizing the MCS. Significant improvement in network performance is observed with higher spatial diversity order and/or erasure insertion decoding. Effects of different Doppler frequency shifts due to mobility and different time-scale of shadowing variation are also evaluated.

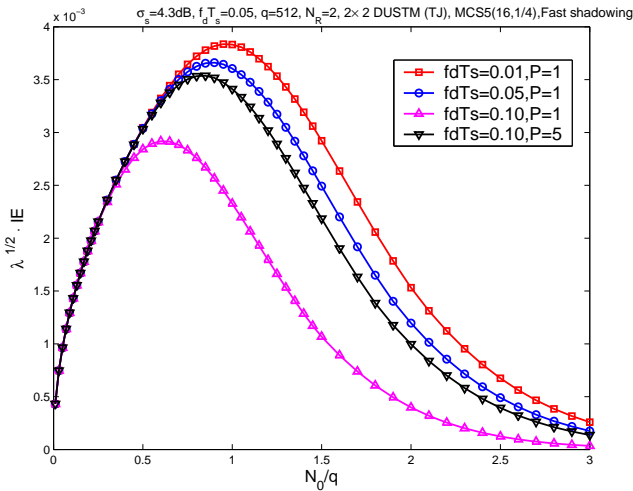


Fig. 5. $\sqrt{\lambda IE}$ versus $\frac{N_0}{q}$ for different mobility and DFD feedback length P ($L = 16$, $K/L = \frac{1}{4}$, $N = 2$, $\sigma_s = 4.3\text{dB}$, fast shadowing)

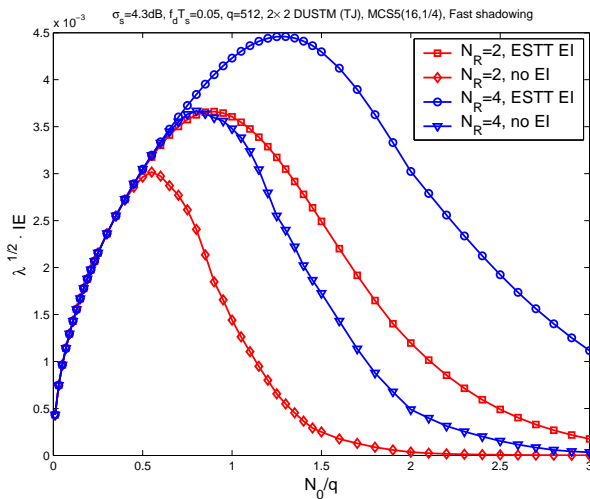


Fig. 6. $\sqrt{\lambda IE}$ versus $\frac{N_0}{q}$ for different receive antenna numbers and with/without EI ($L = 16$, $K/L = \frac{1}{4}$, $\sigma_s = 4.3\text{dB}$, fast shadowing, $fdTs = 0.05$)

REFERENCES

- [1] A. J. Goldsmith, S. B. Wicker, "Design challenges for energy-constrained ad hoc wireless networks," *IEEE Wireless Communications*, Vol.9, No.4, pp.8-27, Aug. 2002
- [2] E. S. Sousa, J. A. Silvester, "Optimum transmission ranges in a direct-sequence spread-spectrum multihop packet radio network," *IEEE J. on Selected Areas of Commun.*, Vol.8, No.5, pp.762-771, Jun. 1990
- [3] M. Zorzi, S. Pupolin, "Optimum transmission ranges in multihop packet radio networks in the presence of fading," *IEEE Trans. Commun.*, Vol.43, No.7, pp.2201-2205, July 1995
- [4] M. W. Chandra, B. L. Hughes, "Optimizing information efficiency in a direct-sequence mobile packet radio network," *IEEE Trans. Commun.*, Vol.51, No.1, pp.22-24, Jan. 2003
- [5] M. W. Subbarao, B. L. Hughes, "Optimal transmission ranges and code rates for frequency-hop packet radio networks," *IEEE Trans. Commun.*, Vol.48, No.4, pp.670-678, Apr. 2000
- [6] P. C.P. Liang, W. E. Stark, "Transmission range control and information efficiency for FH packet radio networks," *Proc. of IEEE Military Commun. Conf. (MILCOM)*, Vol.2, pp.861-865, Oct. 2000
- [7] S. P. Weber, X. Yang, J. G. Andrews, G. de Veciana, "Transmission capacity of wireless ad hoc networks with outage constraints," *IEEE Trans. Info. Theory*, Vol.51, No.12, pp.4091-4102, Dec. 2005
- [8] K. Stamatiou, J. G. Proakis, J. R. Zeidler, "Information efficiency of ad hoc networks with FH-MIMO transceivers," submitted to *IEEE Int. Conf. on Commun. (ICC)*, Jun. 2007
- [9] K. Stamatiou, J. G. Proakis, J. R. Zeidler, "Evaluation of MIMO techniques in FH-MA ad hoc networks," submitted to *IEEE Global Telecommun. Conf. (GLOBECOM)*, Nov. 2007
- [10] H. Sui, J. R. Zeidler, "A robust coded MIMO FH-CDMA transceiver for mobile ad hoc networks," *IEEE J. on Selected Areas of Commun.*, to appear in Sept. 2007
- [11] H. Sui, J. R. Zeidler, "Erasure insertion for coded DUSTM-FHSS systems without a priori knowledge," *Proc. of IEEE Int. Conf. on Commun. (ICC)*, Vol.11, pp.5040-5046, June 2006
- [12] M. Shao, C. L. Nikias, "Signal processing with fractional lower order moments: stable processes and their applications", *Proc. of the IEEE*, Vol.81, No.7, pp.986-1010, Jul. 1993
- [13] E. S. Sousa, "Performance of a spread spectrum packet radio network link in a Poisson field of interferers," *IEEE Trans. Info. Theory*, Vol.38, No.6, pp.1743-1754, Nov. 1992
- [14] J. Ilow, D. Hatzinakos, "Analytic alpha-stable noise modeling in a Poisson field of Interferers or scatterers," *IEEE Trans. Sig. Proc.*, Vol.46, No.6, pp.1601-1611, June 1998
- [15] J. Ilow, D. Hatzinakos, A. N. Venetsanopoulos, "Performance of FH SS radio networks with interference modeled as a mixture of Gaussian and alpha-stable noise," *IEEE Trans. Commun.*, Vol.46, No.4, pp.509-520, Apr. 1998
- [16] V. Tarokh, H. Jafarkhani, "A differential detection scheme for transmit diversity," *IEEE J. Selected Areas Commun.*, Vol.18, No.7, pp. 1169-74, July 2000
- [17] H. Sui, J. R. Zeidler, "An explicit and unified error probability analysis of two detection schemes for differential unitary space-time modulation," *Conf. Record of 39th Asilomar Conf. on Signals, Systems and Computer*, pp.1579-1583, Oct. 2005
- [18] M. Abramowitz, I. A. Stegun, *Handbook of Mathematical Functions with Formulas, Graphs, and Mathematical Tables*, New York: Dover Publications, 1970